International Journal of Robotics and Automation, Vol. 2, No. 2, 1987

OPTIMIZATION OF DYNAMICS IN MANIPULATOR DESIGN: THE OPERATIONAL SPACE FORMULATION

O. Khatib and J. Burdick*

Abstract

In this paper we investigate the dynamic characteristics of manipulators and develop a new method for the optimization of dynamics in manipulator design. The dynamic optimization is aimed here at providing the largest, most isotropic, and most uniform bounds on the magnitude of end-effector acceleration at both low and high velocities. The operational space formulation, which focuses on the dynamic behavior of the manipulator end-effector, forms the basis for this optimization. Using the dynamic model of the end-effector in operational space, we establish the input/output relationship between joint forces and end-effector acceleration in the form of transformation matrices. The joint forces considered here are, more precisely, the available joint forces that can contribute to end-effector acceleration. The design optimization problem is then expressed as a minimization of a cost function with respect to the kinematic, dynamic, and actuator design parameters and their constraints. This cost function is based on the characteristics of the transformation matrices, such as norm and condition number. A simple two-degree-of-freedom mechanism is used to illustrate this formulation.

1. Introduction

The kinematic parameters of a manipulator are among the most significant indices in the evaluation of a manipulator's characteristics. Research on the kinematics of articulated mechanisms has developed means for the analysis of workspace characteristics [15, 17], and the evaluation of kinematic performance [3, 14, 19]. The use of redundancy to improve workspace and singularity characteristics has been investigated [4, 5, 13]. Yoshikawa [19] has proposed a *measure of manipulability* for the evaluation of manipulator kinematic performance. Kinematic and static force characteristics have been also investigated [1].

While in motion, however, manipulators are subject to highly nonlinear inertial, centrifugal, Coriolis, and gravity forces. Characterization of manipulator dynamic performance is, therefore, an essential consideration in the analysis, design, and control of these nonlinear, coupled, and multi-dimensional mechanisms. Asada proposed the generalized inertia ellipsoid [1] as a tool for the characterization of manipulator dynamics and the *measure of manipulability* has been extended to a *measure of dynamic manipulability* [20].

Research in manipulator dynamics has focused on developing the equations of motion in joint space. However, manipulator action is primarily characterized by the motion of the end-effector motion and the forces exerted on the manipulator's environment. The operational space formulation establishes the equations of motion describing end-effector dynamic behavior in the operational space, the space in which the task is originally described. This end-effector dynamic model is a useful tool for the analysis, design and control of manipulator mechanisms with respect to their end-effector dynamic performance.

In this paper, the characterization and optimization of end-effector dynamic performance is based on the end-effector dynamic model. At a given configuration, the dynamic performance is characterized by the magnitude of the "minimum available" isotropic acceleration that is available at the level of the end-effector. Manipulator design optimization is achieved by maximizing this criterion throughout the workspace. This optimization will provide the manipulator with large and uniform bounds on "available operational space forces" throughout the workspace.

Details of the operational space formulation can be found in [7, 8]. After a brief review of this work, the paper will focus on the use of the operational space formulation as a tool for the design of manipulators.

2. Operational Space Formulation

An *operational coordinate system* is a set $\mathbf{x}$ of *m independent* parameters describing the manipulator end-effector position and orientation in a frame of reference R_0. The end-effector equations of motion in operational space can be developed [7, 8] and written in the form

$$\Lambda(\mathbf{x})\ddot{\mathbf{x}} + \mu(\mathbf{x}, \dot{\mathbf{x}}) + \mathbf{p}(\mathbf{x}) = \mathbf{F}; \qquad (1)$$

where $\Lambda(\mathbf{x})$ designates the kinetic energy matrix, and $\mu(\mathbf{x}, \dot{\mathbf{x}})$ represents the vector of end-effector centrifugal and Coriolis forces. $\mathbf{p}(\mathbf{x})$ and $\mathbf{F}$ are respectively the gravity and the generalized operational force vectors.

With respect to a system of n joint coordinates $\mathbf{q}$, the equations of motion in joint space can be written in the form

$$A(\mathbf{q})\ddot{\mathbf{q}} + \mathbf{b}(\mathbf{q}, \dot{\mathbf{q}}) + \mathbf{g}(\mathbf{q}) = \Gamma; \qquad (2)$$

where $\mathbf{b}(\mathbf{q}, \dot{\mathbf{q}})$, $\mathbf{g}(\mathbf{q})$, and Γ, represent the Coriolis and centrifugal, gravity, and generalized forces in joint space; and $A(\mathbf{q})$ is the $n \times n$ joint space kinetic energy matrix, which is related to $\Lambda(\mathbf{x})$ by

$$A(\mathbf{q}) = J^T(\mathbf{q})\Lambda(\mathbf{x})J(\mathbf{q}). \qquad (3)$$

The control of manipulators in operational space is based

*Artificial Intelligence Laboratory, Stanford University, Stanford, California, U.S.A. 94305

on the selection of $\mathbf{F}$ in Equation (1) as a command vector. In order to produce this command, specific forces Γ must be applied with joint-based actuators. With $\mathbf{q}$ representing the vector of n joint coordinates and $J(\mathbf{q})$ the Jacobian matrix, the relationship between $\mathbf{F}$ and the generalized joint forces Γ is given by [10]

$$\Gamma = J^T(\mathbf{q})\mathbf{F}. \tag{4}$$

While in motion, a manipulator end-effector is subject to the highly nonlinear forces mentioned earlier. These nonlinearities can be compensated for by dynamic decoupling in operational space using the end-effector Equations of motion (1). With this decoupling, motion and active force control can be naturally integrated. The unified operational force command vector

$$\mathbf{F} = \mathbf{F}_m + \mathbf{F}_a + \mathbf{F}_{ccg}; \tag{5}$$

where $\mathbf{F}_m$ is the operational command vector for control of end-effector motions, $\mathbf{F}_a$ is the command vector for active control of end-effector forces, and $\mathbf{F}_{ccg}$ are the forces necessary for compensation of centrifugal, Coriolis, and gravity effects. $\mathbf{F}_m$ and $\mathbf{F}_{ccg}$ are given by

$$\begin{aligned} \mathbf{F}_m &= \Lambda(\mathbf{x})\mathbf{F}_m^*; \\ \mathbf{F}_{ccg} &= \mu(\mathbf{x}, \dot{\mathbf{x}}) + \mathbf{p}(\mathbf{x}); \end{aligned} \tag{6}$$

where $\mathbf{F}_m^*$ represents the command vector of the decoupled end-effector, which is equivalent to a decoupled *single unit mass* moving in the m-dimensional space, and $\mathbf{F}_m^*$ is computed using a control law for the decoupled system. For example, a simple motion control law for the decoupled end-effector might be

$$\mathbf{F}_m^* = \ddot{\mathbf{x}}_d + K_v\dot{\mathbf{e}} + K_p\mathbf{e}; \tag{7}$$

where $\ddot{\mathbf{x}}_d$ is the desired end-effector acceleration, $\mathbf{e}$ and $\dot{\mathbf{e}}$ are the errors in end-effector position and velocity, and K_v and K_p are diagonal matrices of velocity and position error gains. Alternatively, more complex and nonlinear control laws, such as sliding mode control [18], can be used to compute $\mathbf{F}_m^*$ within this framework. Using Equation (4), the joint forces corresponding to the operational command vector $\mathbf{F}$ in (6) can be written as

$$\Gamma = J^T(\mathbf{q})\left[\Lambda(\mathbf{q})\mathbf{F}_m^* + \mathbf{F}_a\right] + \tilde{\mathbf{b}}(\mathbf{q}, \dot{\mathbf{q}}) + \mathbf{g}(\mathbf{q}); \tag{8}$$

where $\tilde{\mathbf{b}}(\mathbf{q}, \dot{\mathbf{q}})$ is the vector of end-effector Coriolis and centrifugal forces, $\mu(\mathbf{x}, \dot{\mathbf{x}})$, mapped back into joint space. In order to simplify the notation, Λ has been also used here to designate the kinetic energy matrix when expressed as a function of the joint coordinate vector $\mathbf{q}$. The vector $\tilde{\mathbf{b}}(\mathbf{q}, \dot{\mathbf{q}})$ is *distinct* from the vector of centrifugal and Coriolis forces, $\mathbf{b}(\mathbf{q}, \dot{\mathbf{q}})$, that arise when viewing the manipulator motion in joint space. These vectors are related by

$$\tilde{\mathbf{b}}(\mathbf{q}, \dot{\mathbf{q}}) = \mathbf{b}(\mathbf{q}, \dot{\mathbf{q}}) - J^T(\mathbf{q})\Lambda(\mathbf{q})\mathbf{h}(\mathbf{q}, \dot{\mathbf{q}}); \tag{9}$$

where

$$\mathbf{h}(\mathbf{q}, \dot{\mathbf{q}}) = \dot{J}(\mathbf{q})\dot{\mathbf{q}}. \tag{10}$$

$\tilde{\mathbf{b}}(\mathbf{q}, \dot{\mathbf{q}})$ can be expressed in the following form (which will be useful in Section 4)

$$\tilde{\mathbf{b}}(\mathbf{q}, \dot{\mathbf{q}}) = \tilde{B}(\mathbf{q})[\dot{\mathbf{q}}\dot{\mathbf{q}}] + \tilde{C}(\mathbf{q})[\dot{\mathbf{q}}^2]; \tag{11}$$

where $\tilde{B}(\mathbf{q})$ and $\tilde{C}(\mathbf{q})$ are the $n \times n(n-1)/2$ and $n \times n$ matrices of end-effector Coriolis and centrifugal forces mapped into joint space. $[\dot{\mathbf{q}}\dot{\mathbf{q}}]$ and $[\dot{\mathbf{q}}^2]$ are the symbolic notations for the $n(n-1)/2 \times 1$ and $n \times 1$ column matrices

$$\begin{aligned} [\dot{\mathbf{q}}\dot{\mathbf{q}}] &= [\dot{q}_1\dot{q}_2\dot{q}_1\dot{q}_3 \cdots \dot{q}_n - 1\dot{q}_n]^T; \\ [\dot{\mathbf{q}}^2] &= [\dot{q}_1^2\dot{q}_2^2 \cdots \dot{q}_n^2]^T. \end{aligned}$$

This approach to manipulator motion and active force control has been implemented in an experimental manipulator programming system COSMOS. Using a PUMA 560, demonstrations of real-time end-effector motion and active force control operations have been performed [11, 12], as well as real-time collision avoidance [9].

3. Characterization of End-Effector Dynamic Performance

When evaluating the dynamic performance of a manipulator, we are primarily concerned with the dynamic characteristics of the end-effector in the manipulator workspace. In this section we consider the relationship between the operational space control system and end-effector dynamic behavior and show how end-effector acceleration performance is one of the most important characteristics in the evaluation of the manipulator dynamic behavior.

Let us examine the operational command vector $\mathbf{F}_m$ in (6), which achieves the dynamic decoupling and motion control of end-effector motion. Only a fraction of these operational forces, specifically $\mathbf{F}_m^*$, contribute to the end-effector acceleration and the control of end-effector motion. $\mathbf{F}_m^*$ can be seen as the input of the decoupled end-effector, which is equivalent to a single unit mass. The rest of the operational forces are used for nonlinear compensation and dynamic decoupling.

The end-effector dynamic performance of the manipulator under control is, therefore, strongly dependent on the extent of the boundaries of $\mathbf{F}_m^*$. As will be shown below, limits on $\mathbf{F}_m^*$ are equivalent to limits on the magnitude of available end-effector acceleration. Boundaries on $\mathbf{F}_m^*$ are analogous to the saturation of actuators. From Equation (7), it can easily be seen that bounds on $\mathbf{F}_m^*$ will limit the maximum position error gains that can be used in normal operation before the limits of $\mathbf{F}_m^*$ are reached. By achieving large and isotropic bounds on $\mathbf{F}_m^*$ throughout the manipulator workspace, closed loop manipulator response and disturbance rejection can be improved.

Using the dynamic model in (1), end-effector acceleration is given by

$$\ddot{\mathbf{x}} = \Lambda^{-1}(\mathbf{x})[\mathbf{F} - \mu(\mathbf{x}, \dot{\mathbf{x}}) - \mathbf{p}(\mathbf{x})]. \qquad (12)$$

This equation relates end-effector acceleration to generalized applied end-effector forces (corrected for gravity, centrifugal and Coriolis forces) through the inverse of the operational space kinetic energy matrix. Asada [1] has used this matrix in formulating the Generalized Inertia Ellipsoid (GIE) for the characterization of manipulator dynamics.

The GIE has been viewed as a tool for manipulator dynamic optimization to provide uniform and isotropic inertia characteristics throughout the manipulator workspace. Although the GIE establishes the relationship between end-effector forces and accelerations, this relationship does not relate actual actuator force input to end-effector accelerations. The forces involved in (12) are the generalized operational forces F acting at the end-effector. However, end-effector operational control forces are produced by joint actuators through the inverse of Equation (4). The bounds on end-effector forces are therefore configuration dependent, and do not represent an isotropic and uniform input in Equation (12). Thus, a uniform GIE does not guarantee uniform end-effector acceleration performance.

Since desired end-effector motions and applied forces are specified in orthogonal subspaces of the operational space [11], the evaluation of the uniformity and isotropicity of end-effector behavior requires an independent analysis for motion and force control throughout the operational space. For the moment, let us consider end-effector performance under motion control. For end-effector motion performance, the relationship between $\mathbf{F}_m^*$ and joint forces can be obtained from (8) as

$$\mathbf{F}_m^* = E(\mathbf{q})[\Gamma - \tilde{\mathbf{b}}(\mathbf{q}, \dot{\mathbf{q}}) - \mathbf{g}(\mathbf{q})]; \qquad (13)$$

where

$$E(\mathbf{q}) = [J^T(\mathbf{q})\Lambda(\mathbf{q})]^{-1}. \qquad (14)$$

For non-redundant manipulators, $E(\mathbf{q})$ can be written as $J(\mathbf{q})A^{-1}(\mathbf{q})$. Since $\mathbf{F}_m^*$ is equivalent to the acceleration of the decoupled unit mass end-effector, $E(\mathbf{q})$ also establishes the relationship between joint forces and end-effector accelerations (using equations (4) and (12))

$$\ddot{\mathbf{x}} = E(\mathbf{q})[\Gamma - \tilde{\mathbf{b}}(\mathbf{q}, \dot{\mathbf{q}}) - \mathbf{g}(\mathbf{q})]. \qquad (15)$$

Thus, bounds on $\mathbf{F}_m^*$ are equivalent to bounds on $\ddot{\mathbf{x}}$.

The *measure of dynamic manipulability* proposed by Yoshikawa [20] is based on the matrix $E(\mathbf{q})$. The input/output relationship in Yoshikawa's formulation relates the manipulator generalized forces Γ corrected for gravity $\mathbf{g}(\mathbf{q})$ and the joint space centrifugal and Coriolis forces $\mathbf{b}(\mathbf{q}, \dot{\mathbf{q}})$ to a "pseudo" acceleration vector. This vector consists of the actual end-effector acceleration corrected for the vector $\mathbf{h}(\mathbf{q}, \dot{\mathbf{q}})$ of (10), which has been interpreted as a virtual acceleration. However, as shown in Equation (10), this vector is part of the expression $\tilde{\mathbf{b}}(\mathbf{q}, \dot{\mathbf{q}})$, and so the use of the *dynamic manipulability* measure does not correctly evaluate end-effector acceleration performance at non-zero velocity.

For the performance analysis of end-effector applied forces, only static forces are significant, and the relevant relationship can be established with respect to the desired applied forces $\mathbf{F}_d$ as

$$\mathbf{F}_d = J^{-T}(\mathbf{q})[\Gamma - \mathbf{g}(\mathbf{q})]. \qquad (16)$$

Equations (15) and (16) establish the basic relationship between joint forces and end-effector motions and applied forces. In the following sections, we will concentrate on manipulator dynamic optimization with respect to end-effector motion performance.

4. Formulation of End-Effector Dynamic Characterization

The mapping of joint forces to end-effector accelerations is illustrated in Fig. 1 for a planar manipulator with two revolute joints. When operating in the horizontal plane, and at zero velocity, the bounds on end-effector acceleration are given by the mapping of the bounds on joint actuator torques through the relation

$$\ddot{\mathbf{x}} = E(\mathbf{q})\Gamma;$$

as shown for a given configuration, $\mathbf{q}$, in Fig. 1. Fig. 2 shows how these bounds vary as a function of the manipulator's configuration.

When operating in the vertical plane, so that gravitational effects are present, the relationship between end-effector accelerations and joint torques is

$$\ddot{\mathbf{x}} = E(\mathbf{q})[\Gamma - \mathbf{g}(\mathbf{q})].$$

Gravitational forces will modify the bounds on the joint torques that are able to affect accelerations of the end-effector. This is shown in Fig. 3, where the dashed lines represent actuator bounds, while the solid lines represent the effective joint forces. At a given configuration, end-effector dynamic performance can be characterized by the

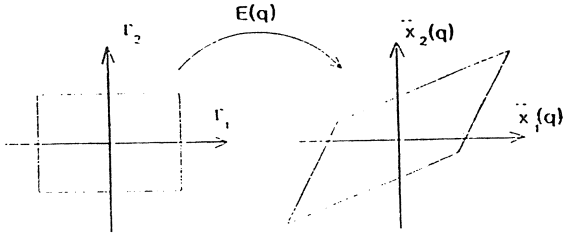

Figure 1. End-effector acceleration bounds.

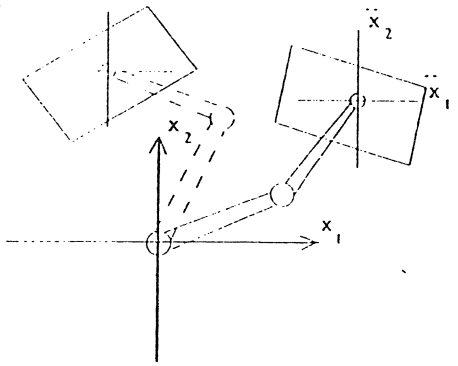

Figure 2. The configuration dependency of acceleration bounds.

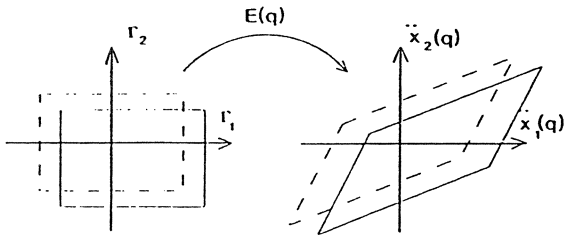

Figure 3. Gravitational effects on the acceleration bounds.

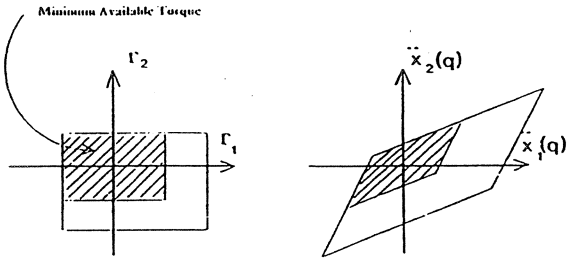

Figure 4. Minimum available acceleration.

"minimum available" end-effector acceleration. This acceleration, as illustrated in Fig. 4, is limited by the minimum available joint torques that are able to contribute to end-effector acceleration.

Let $\underline{\Gamma}_{0_i}$ and $\overline{\Gamma}_{0_i}$ be respectively the minimal and maximal bounds of the i^{th} actuator force Γ_i at zero joint velocity. At a given configuration, $\mathbf{q}$, the minimal value of the amplitude of the i^{th} joint force that is available to contribute to the end-effector acceleration at zero joint velocity is given by

$$\gamma_{0_i}(\mathbf{q}) = \min\left(|\underline{\Gamma}_{0_i} - g_i(\mathbf{q})|, |\overline{\Gamma}_{0_i} - g_i(\mathbf{q})|\right); \quad (17)$$

where γ_{0_i} is the minimum available torque described above. Using these minimum available joint forces, let us define an $n \times n$ joint force normalization matrix,

$$N_0(\mathbf{q}) = \mathrm{diag}\left(\gamma_{0_i}(\mathbf{q})\right); \quad (18)$$

so that the vector of normalized joint forces that are able to contribute to end-effector acceleration is confined to the unit hypercube $\mathscr{D}_f$

$$\mathscr{D}_f = N_0^{-1}(\mathbf{q}) \prod_{i=1}^{n} \left[-\gamma_{0_i}(\mathbf{q}), \gamma_{0_i}(\mathbf{q})\right]. \quad (19)$$

Define the $m \times m$ acceleration weighting matrix W

$$W = \begin{pmatrix} I_{m_p} & 0 \\ 0 & wI_{m_r} \end{pmatrix}; \quad (20)$$

where I_{m_p}, I_{m_r}, and 0 are the identity and zero matrices with the dimensions of the end-effector position and orientation sub-spaces, m_p and m_r. w is a "metric homogeneity" weighting coefficient between the linear and angular accelerations of the end-effector. This weighting is introduced to normalize angular accelerations with respect linear accelerations. The minimum available weighted acceleration $W\ddot{\mathbf{x}}$ at zero joint velocities is then within the hyperparallelepiped $\mathscr{D}_{a_0}$

$$\mathscr{D}_{a_0} = E_0(\mathbf{q})\mathscr{D}_f; \quad (21)$$

where

$$E_0(\mathbf{q}) = WE(\mathbf{q})N_0(\mathbf{q}). \quad (22)$$

The matrix $E_0(\mathbf{q})$ describes the mapping, at zero joint velocities, of the unit hypercube of normalized joint forces (19) into the hyperparallelepiped of weighted accelerations (21). For a given manipulator, $E_0(\mathbf{q})$ incorporates the effects of gravity and joint torque limits and is a transmission matrix that characterizes the dynamic performance of the manipulator at zero velocity.

Coriolis and centrifugal forces which arise at non-zero joint velocities modify the values of minimum available joint forces. In typical robotic actuators (such as D.C. servo motors), the actuator force bounds are similarly modified at high velocities. Let $\bar{\dot{\mathbf{q}}}$ be the vector of maximum operating joint velocities, and let us designate by $\underline{\Gamma}_{v_i}$ and $\overline{\Gamma}_{v_i}$ the lower and upper bounds of the i^{th} actuator force Γ_i at these maximum velocities. The minimal value of the amplitude of i^{th} joint force that is available to contribute to the end-effector acceleration at $\bar{\dot{\mathbf{q}}}$ becomes

$$\gamma_{v_i}(\mathbf{q}) = \min\left(|\underline{\sigma}_i(\mathbf{q}) - \mathrm{sign}(\bar{\sigma}_i)\nu_i(\mathbf{q})|, |\bar{\sigma}_i(\mathbf{q}) - \mathrm{sign}(\bar{\sigma}_i)\nu_i(\mathbf{q})|\right); \quad (23)$$

where $\underline{\sigma}_i$, $\bar{\sigma}_i$, and ν_i are the i^{th} components of the vectors

$$\begin{aligned} \underline{\sigma}(\mathbf{q}) &= \underline{\Gamma}_v - \mathbf{g}(\mathbf{q}) - \tilde{C}(\mathbf{q})\left[\bar{\dot{\mathbf{q}}}^2\right]; \\ \bar{\sigma}(\mathbf{q}) &= \overline{\Gamma}_v - \mathbf{g}(\mathbf{q}) - \tilde{C}(\mathbf{q})\left[\bar{\dot{\mathbf{q}}}^2\right]; \\ \nu(\mathbf{q}) &= \mathscr{A}\left(\tilde{B}(\mathbf{q})\right)\left[\bar{\dot{\mathbf{q}}}\bar{\dot{\mathbf{q}}}\right]. \end{aligned} \quad (24)$$

The operator $\mathscr{A}$ produces the matrix of the absolute values of the elements of $\tilde{B}(\mathbf{q})$. $\nu_i(\mathbf{q})$ therefore represents the largest absolute values of Coriolis force that can occur

at the i^{th} joint during any motion within the limits of maximum operating joint velocities. At these velocities, the joint force normalization matrix and the hyperparallelepiped of minimum available weighted end-effector acceleration become

$$N_v(\mathbf{q}) = \mathrm{diag}\big(\gamma_{v_i}(\mathbf{q})\big);$$
$$\mathscr{D}_{a_v} = E_v(\mathbf{q})\mathscr{D}_f; \tag{25}$$

where

$$E_v(\mathbf{q}) = WE(\mathbf{q})N_v(\mathbf{q}). \tag{26}$$

$E_v(\mathbf{q})$ characterizes the dynamic behavior of the manipulator at its maximum operating velocity.

5. Optimization of Dynamic Performance

In manipulator design using the operational space approach, dynamic optimization is aimed at providing the largest and the most isotropic and uniform bounds on the end-effector acceleration, or equivalently, on the command vector $\mathbf{F}_m^*$ (6), at both low and high velocities. While performance at high velocities is important in fast gross motion operations, performance at low velocities is particularly important for fast response in tasks with a relatively smaller range of motion or during assembly operations involving the active force control of contact forces. The $E_0(\mathbf{q})$ and $E_v(\mathbf{q})$ matrices establish the input/output relationship between the minimum available joint forces and the end-effector weighted accelerations at zero and maximum joint velocities.

In a given configuration $\mathbf{q}$, the $E_0(\mathbf{q})$ and $E_v(\mathbf{q})$ matrices are expresssed as a function of the manipulator's kinematic, dynamic, and actuator parameters; e.g. link lengths, masses, inertias, centers of mass, actuator masses, and their force and velocity limits. Let η designate the set of these parameters.

In the manipulator design process, workspace and kinematic considerations will be used first to determine the set of possible kinematic configurations of the mechanism. The kinematic parameters associated with each of these kinematic configurations will be specified within some design boundaries. These kinematic specifications, in addition to dynamic and structure requirements, establish various constraints on some or all of the manipulator design parameters η. Kinematic, dynamic, and actuator parameters are in fact highly interconnected. For example, the link's mass, center of mass, and inertias are affected by the variations of its length or actuator force specifications. Let $\{u_i(\eta);\ i = 1,\ldots,n_u\}$ and $\{v_i(\eta);\ i = 1,\ldots,n_v\}$ designate the sets of equality and inequality constraints on the manipulator design parameters η.

The optimization problem can then be formalized in terms of finding the design parameters η, under the constraints $\{u_i(\eta)\}$ and $\{v_i(\eta)\}$, that maximize the volume of the hyperparallelepipeds $\mathscr{D}_{a_0}$, $\mathscr{D}_{a_v}$ and minimize the ratio of their largest and smallest axes. Expressed as a function of the manipulator configuration $\mathbf{q}$ and the design parameters η, the matrices $E_0(\mathbf{q}, \eta)$ and $E_v(\mathbf{q}, \eta)$ constitute the basic components in this optimization problem.

The matrices $E_0(\mathbf{q}, \eta)$ and $E_v(\mathbf{q}, \eta)$ are asymmetric. However, using the polar decomposition, an $m \times n$ asymmetric matrix M can be represented as the product of an orthogonal matrix, U, with the symmetric positive semi-definite matrix $\sqrt{(MM^T)}$. The orthogonal matrix in this decomposition describes the rotation properties of vectors mapped by M while $\sqrt{(MM^T)}$ contains the elongation characteristics of these mapped vectors. The largest eigenvalue of $\sqrt{(MM^T)}$ is in fact the Euclidean norm $\|M\|$ of M. In addition, the ratio of this eigenvalue to the smallest one, *i.e.* the *condition number* $\kappa(M)$, characterizes the uniformity of the mapping by M. The condition number has been used to evaluate the kinematic characteristics in articulated hand design [16].

Finally, the problem of dynamic optimization over the manipulator work space $\mathscr{D}_q$ can be expressed as the minimization of a global cost function $\tilde{C}(\eta)$

$$\min \tilde{C}(\eta) = \min \int_{\mathscr{D}_q} C(\mathbf{q}, \eta) w(\mathbf{q}) d\mathbf{q}$$

subject to the constraints

$$u_i(\eta) = 0 \qquad i = 1,\ldots,n_u;$$
$$v_i(\eta) \le 0 \qquad i = 1,\ldots,n_v; \tag{27}$$

where the function $w(\mathbf{q})$ is used to relax the weighting of the local cost function $C(\mathbf{q}, \eta)$ in the vicinity of the work space boundaries and singularities. This local cost function is composed of terms involving the magnitude and isotropicity characteristics at a given configuration, and is given by

$$C(\mathbf{q}, \eta) = \left[\frac{1}{\|E_0(\mathbf{q}, \eta)\|} + \alpha_0 \kappa\big(E_0(\mathbf{q}, \eta)\big)\right] + w_v\left[\frac{1}{\|E_v(\mathbf{q}, \eta)\|} + \alpha_v \kappa\big(E_v(\mathbf{q}, \eta)\big)\right]. \tag{28}$$

$\alpha_0(\alpha_v)$ is the desired relative weighting between the end-effector acceleration characteristics of isotropicity and magnitude at zero velocity (maximum operating velocity). w_v controls the relative importance given to dynamic performance at high velocity.

The optimization of manipulator performance for tasks involving applied end-effector forces can be similarly formulated, using the relation (16). In addition, the optimization of end-effector velocity performance can also be formulated using the manipulator kinematic model and the actuator velocity characteristics. In the manipulator design process, end-effector dynamic, applied force, and kine-

matic performance can be incorporated into a global optimization by extending the previous cost function.

6. Application

In the following example, simple two-link arm is used to illustrate this formulation for the dynamic optimization of manipulator systems. Both joints are assumed to be revolute and to have parallel axes of rotation. Let l_i, m_i, $\mathbf{r}_i$, and I_i be the length, mass, distance vector from the joint to the center of mass, and the inertia at the center of mass for the i^{th} link. Gravity acts in the plane perpendicular to these axes. If s_1, c_1, s_2, c_2, s_{12}, and c_{12} denote respectively, $\sin(q_1)$, $\cos(q_1)$, $\sin(q_2)$, $\cos(q_2)$, $\sin(q_1 + q_2)$, and $\cos(q_1 + q_2)$, the Jacobian matrix for this manipulator, expressed in the base reference frame coordinates, is

$$J = \begin{pmatrix} -l_1 s_1 - l_2 s_{12} & -l_2 s_{12} \\ l_1 c_1 + l_2 c_{12} & l_2 c_{12}. \end{pmatrix} \tag{29}$$

The elements of the operational space kinetic energy matrix $\Lambda(\mathbf{q})$ are

$$\begin{aligned} \lambda_{11} &= \left[\left(\tilde{I}_1 - \tilde{I}_2 + m_2 l_1^2\right) l_2^2 - 2\left(\tilde{I}_2 + k_1\right) l_1 l_2 c_2 \right. \\ &\qquad \left. + \tilde{I}_2 l_1^2 s_2^2\right] / (l_1 l_2 s_2)^2; \\ \lambda_{12} &= \left(k_1 l_2 - \tilde{I}_2 l_1 c_2\right) / l_1 l_2^2 s_2; \\ \lambda_{22} &= \tilde{I}_2 / l_2^2; \\ \lambda_{21} &= \lambda_{12}; \end{aligned} \tag{30}$$

where

$$\begin{aligned} \tilde{I}_1 &= I_1 + m_1\left(r_{x_1}^2 + r_{y_1}^2\right); \\ \tilde{I}_2 &= I_2 + m_2\left(r_{x_2}^2 + r_{y_2}^2\right); \\ k_1 &= m_2 l_1 (r_{x_2} c_2 - r_{y_2} s_2). \end{aligned}$$

The elements of the matrices $\tilde{B}(\mathbf{q})$ and $\tilde{C}(\mathbf{q})$ are

$$\begin{aligned} \tilde{b}_{11} &= -2k_2 - 2\lambda_{11} y_1 x_2 \\ &\qquad + 2\lambda_{12}(x_1 x_2 - y_1 y_2) + 2\lambda_{22} x_1 y_2; \\ \tilde{b}_{12} &= 2(\lambda_{22} - \lambda_{11}) x_2 y_2 + 2\lambda_{12}\left(x_2^2 - y_2^2\right); \end{aligned} \tag{31}$$

and

$$\begin{aligned} \tilde{c}_{11} &= (\lambda_{22} - \lambda_{11}) x_1 y_1 + \lambda_{12}\left(x_1^2 - y_1^2\right); \\ \tilde{c}_{12} &= -k_2 - \lambda_{11} y_1 x_2 + \lambda_{12}(x_1 x_2 - y_1 y_1) + \lambda_{22} y_1 x_2; \\ \tilde{c}_{21} &= k_2 - \lambda_{11} x_1 y_2 + \lambda_{12}(x_1 x_2 - y_1 y_2) + \lambda_{22} y_1 x_2; \\ \tilde{c}_{22} &= (\lambda_{22} - \lambda_{11}) x_2 y_2 + \lambda_{12}\left(x_2^2 - y_2^2\right); \end{aligned} \tag{32}$$

where

$$\begin{aligned} k_2 &= m_2 l_1 (r_{x_2} s_2 + r_{y_2} c_2); \\ x_1 &= l_1 c_1 + l_2 c_{12}; \\ y_1 &= l_1 s_1 + l_2 s_{12}; \\ x_2 &= l_2 c_{12}; \\ y_2 &= l_2 s_{12}. \end{aligned}$$

With g representing the acceleration of gravity, the components of the gravity vector $\mathbf{g}(\mathbf{q})$ are

$$\begin{aligned} g_2 &= m_2 (r_{x_2} c_{12} - r_{y_2} s_{12}) g; \\ g_1 &= g_2 + m_1 (r_{x_1} c_1 - r_{y_1} s_1) g + m_2 l_1 c_1 g. \end{aligned} \tag{33}$$

In this example, the link lengths are constrained to maintain a maximum extension of l_{max}, while link each length is constrained to be within the range of $\underline{l}$ to $\bar{l}$. These constraint equations are simply expressed as

$$\begin{aligned} l_1 + l_2 &= l_{max}; \\ l_i &\geq \underline{l}; \\ l_i &\leq \bar{l}; \end{aligned} \tag{34}$$

For this example, $l_{max} = 1.0$ meter, $\underline{l} = 0.4$ meter, and $\bar{l} = 0.6$ meter.

In order to illustrate the type of constraints that might arise on the manipulator dynamic parameters, suppose that each link is constructed as a solid cylinder, and that the actuators are located at the joints. The minimum value of the link cylinder radius can be expressed as a function of the maximum loading force f_{max}, the allowable structural stress in the links ζ (which can be related to the maximum link deflection under load), the length of the link, and the material properties of the link. Consequently, link masses and inertias will be constrained by the value of the minimum link radius. For this example, the constraints on the mass and inertia are

$$\begin{aligned} m_i &\geq k l_i^{5/3} + m_{a_i}; \\ I_i &\geq \frac{k}{3}\left(l_i^2 - 3 l_i r_{x_i} + 3 r_{x_i}^2\right) l_i^{5/3} + I_{a_i} + m_{a_i} r_{x_i}^2; \end{aligned} \tag{35}$$

where

$$k = \rho (4 f_{max} / \pi \zeta)^{2/3};$$

ρ = is the material density of the link structural material

and m_{a_i} and I_{a_i} are the mass and Inertia of the i^{th} actuator. Actuators are assumed to have symmetrical peak torques ($\bar{\Gamma}_{0_i} = -\underline{\Gamma}_{0_i}$), and their masses and inertias are considered to be linearly proportional to the peak torque

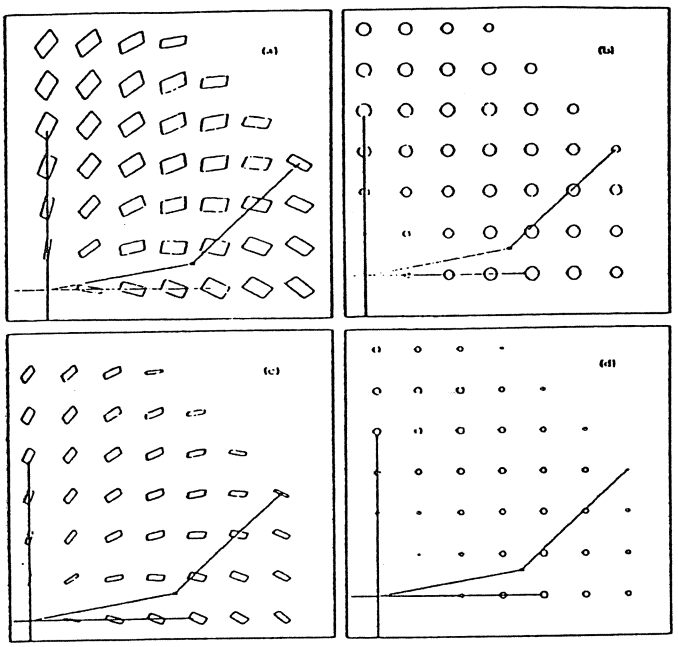

$l_1 = 0.5m, m_1 = 12.5kg, r_{x_1} = 0.25m, r_{y_1} = 0, I_1 = 1.602kg \cdot m^2$

$l_2 = 0.5m, m_2 = 9.5kg, r_{x_2} = 0.25m, r_{y_2} = 0, I_2 = 0.664kg \cdot m^2$

$\bar{\Gamma}_{0_1} = 500Nm, \bar{\Gamma}_{v_1} = 350Nm, \bar{\Gamma}_{0_2} = 200Nm, \bar{\Gamma}_{v_2} = 140Nm$

Figure 5. Initial design.

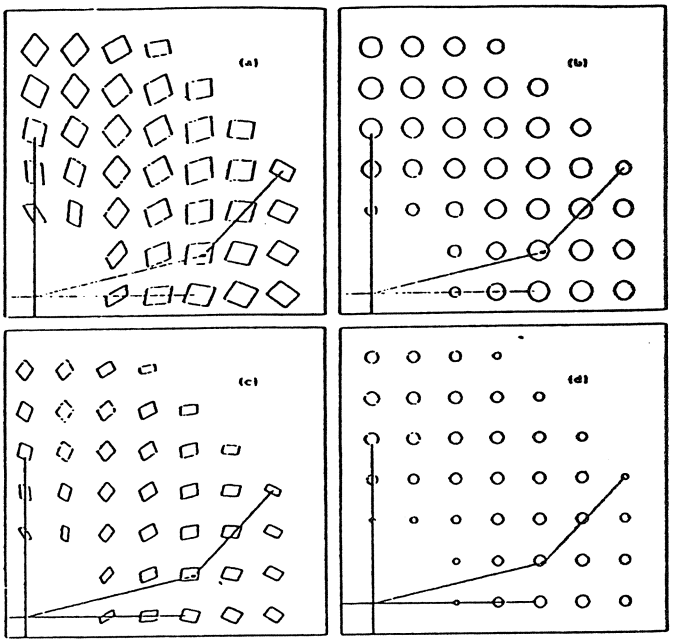

$l_1 = 0.60m, m_1 = 16.92kg, r_{x_1} = 0.20m, r_{y_1} = 0, I_1 = 1.93kg \cdot m^2$

$l_2 = 0.4m, m^2 = 6.09kg, r_x^2 = 0.21m, r_{y_2} = 0, I_2 = 0.39kg \cdot m^2$

$\bar{\Gamma}_{0_1} = 612Nm, \bar{\Gamma}_{v_1} = 428Nm, \bar{\Gamma}_{0_2} = 130Nm, \bar{\Gamma}_{v_2} = 91Nm$

Figure 6. Optimized design.

magnitude

$$m_{a_i} = k_{a_m} \bar{\Gamma}_{0_i} I_{a_i} = k_{a_i} \bar{\Gamma}_{0_i}; \quad (36)$$

where k_{a_m} and k_{a_i} are the proportionality coefficients of actuator masses and inertias. In addition, the joint torques $\underline{\Gamma}_{v_i}$ and $\bar{\Gamma}_{v_i}$ at maximum operating joint velocities (2.0 rad/sec) are reduced to 70% of their values at zero velocity ($\underline{\Gamma}_{0_i}$, $\bar{\Gamma}_{0_i}$).

The set of design parameters η consists of $\{l_i, m_i, I_i, r_{x_i}, m_{a_i}, I_{a_i}, \underline{\Gamma}_{0_i}, \bar{\Gamma}_{0_i}\}$, while the equality and inequality constraints are represented by Equations (34), (35), and (36). In this example, the selected material is steel ($\rho = 7880kg/m^3$), $f_{max} = 650N$, $\zeta = 68.9\ 10^6 N/m^2$, and the motor mass and inertia proportionality constants ($k_{a_m} = 0.01$, $k_{a_i} = 0.0025$) are representative of typical high performance D.C. servo motors.

Initial Design from Joint Space Perspective

Figs. 5 and 6 illustrate the dynamic performance for two different arm designs. The parallelepipeds in the upper left figures (a) depict the boundaries on minimum available end effector acceleration at zero joint velocities. The largest circles that can be inscribed within these boundaries, which represent the magnitude of the minimum available isotropic accelerations, are shown in the upper right figures (b) (A more detailed drawing of the minimum isotropically available acceleration and its relation to acceleration bounds is shown in Fig. 7). The lower figure (c, d) illustrate these accelerations at maximum operating joint velocities. Let $\bar{a}_0$ and $\bar{a}_v$ be the average magnitude of available isotropic acceleration over the workspace at zero and maximum joint operating velocities, respectively.

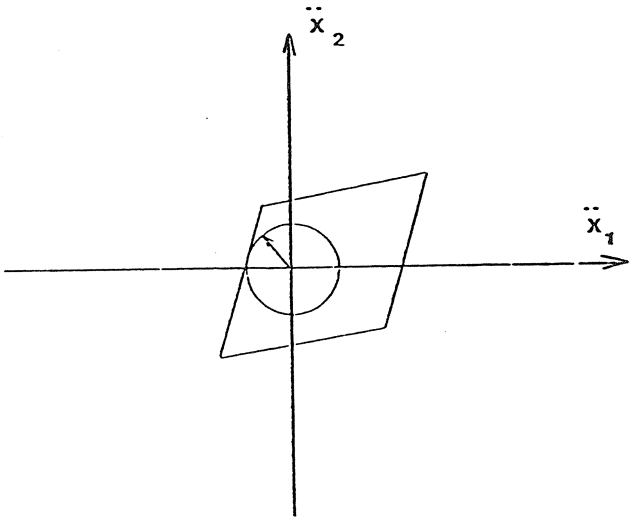

Figure 7. Minimum isotropic acceleration.

The dynamic performance shown in Fig. 4 corresponds to an initial set of design parameters that were developed using only joint space, rather than operational space, considerations. Kinematically, the optimum link lengths occur at $l_1 = l_2 = 0.5$ m. Using these link lengths, the minimum

link radii, mass and inertia were calculated, and the actuators were sized to be based on gravity loading and uniform joint space acceleration considerations. However, this design yields poor isotropic end effector acceleration characteristic. In addition, the magnitude of the minimum available acceleration at maximum operating velocity is appreciably reduced. $\bar{a}_0$ and $\bar{a}_v$ are 38.3 m/sec^2 and 19.0 m/sec^2, respectively.

Optimized Design

The design parameters of the above arm were used as the starting point for a gradient search algorithm which used the cost function given in Equation (27), and the constraints in Equations (34), (35), and (36). Fig. 6 shows the results of the optimization. At zero velocity, $\bar{a}_0$ is 59.7 m/sec^2, which represents an improvement of 56% over the initial design. More significantly, at maximum velocity $\bar{a}_v$ is 35.1 m/sec^2, an increase of 85% relative to the initial arm. The sum of the actuator torques required in this improved design are only 6.0% higher than those used in the initial design.

7. Conclusion

The dynamic optimization problem in manipulator design has been formalized, using the end-effector equations of motion in operational space. The characteristics of the relationship that governs the transfer of joint forces to end-effector accelerations have been used for the evaluation of the manipulator dynamic performance. The optimization problem has been expressed as the minimization, with respect to the design parameters and constraints, of a cost function based on these characteristics.

The large isotropic and uniform bounds on end-effector acceleration provided by this dynamic optimization will be translated into a large and well conditioned operational space command vector. This will provide the control system, in addition to the forces necessary for end-effector dynamic decoupling, sufficient operational forces to achieve the desired design performance throughout the workspace.

The kinematic characterization and optimization of manipulators can be similarly formulated. A global optimization integrating kinematic and dynamic criterion can be achieved.

Acknowledgements

The support from the National Science Foundation and the Systems Development Foundation are gratefully ackowledged. Bradley Chen's assistance in the graphical illustrations is appreciated.

References

[1] Asada, H., "A Geometrical Representation of Manipulator Dynamics and Its Application to Arm Design", *Trans. of ASME, Journal of Dynamic Systems, Measurement, and Control*, Vol. 105, No. 3, September 1983, pp. 131–135.

[2] Asada, H. and Granito, J.A., "Kinematic and Static Characterization of Wrist Joints and Their Optimal Design", *Proceedings of the 1985 International Conference on Robotics and Automation*, St. Louis, March 1985, pp. 244–250.

[3] Fournier, A., "Génération de Mouvements en Robotique. Application des Inverses Généralisées et des Pseudo Inverses", *Thèse d'Etat*, Mention Science, Université des Sciences et Techniques des Languedoc, Montpellier, France, April 1980.

[4] Hanafusa, H., Yoshikawa, T., and Nakamura, Y., 1981. "Analysis and Control of Articulated Robot Arms with Redundancy", *8th IFAC World Congress*, Vol. XIV, 1981, pp. 38–83.

[5] Hollerbach, J.M., "Optimum Kinematic Design for a Seven Degree of Freedom Manipulator", *Prep. of the 2nd International Symposium of Robotics Research*, Kyoto, Japan, August 1984, pp. 349–356.

[6] Khatib, O. and Le Maitre, J.F., "Dynamic Control of Manipulators Operating in a Complex Environment", *Proceedings Third CISM-IFToMM Symposium on Theory and Practice of Robots and Manipulators*, Udine, Italy, September 1978, pp. 267–282.

[7] Khatib, O., "Commande Dynamique dans l'Espace Opérationnel des Robots Manipulateurs en Présence d'Obstacles", *Thése de Docteur-Ingénieur*, École Nationale Supérieure de l'Aéronautique et de l'Espace (ENSAE), Toulouse, France, 1980.

[8] Khatib, O., "Dynamic Control of Manipulators in Operational Space", *Sixth CISM-IFToMM Congress on Theory of Machines and Mechanisms*, New Delhi, India, December 1983, pp. 1128–1131.

[9] Khatib, O., "Real-Time Obstacle Avoidance for Manipulators and Mobile Robots", *Proceedings of the 1985 International Conference on Robotics and Automation*, St. Louis, March 1985, pp. 500–505. Louis.

[10] Khatib, O., "A Unified Approach to Motion and Force Control of Robot Manipulators: The Operational Space Formulation", *IEEE Journal of Robotics and Automation*, Vol. 3, No. 1, 1987, pp. 43–53.

[11] Khatib, and Burdick, J., "Motion and Force Control of Robot Manipulators", *Proceedings of the 1986 IEEE International Conference on Robotics and Automation*, San Francisco, April 1986, pp. 1381–1386.

[12] Khatib, O., Burdick, J. and Armstrong, B., "Robotics in Three Acts - Part II" (Film), Artificial Intelligence Laboratory, Stanford University, 1985.

[13] Luh, J.Y.S. and Gu, Y.L., "Industrial Robots With Seven Joints", *Proceedings 1985 IEEE International Conference on Robotics and Automation*, St. Louis, March 1985, pp. 1010–1015.

[14] Paul, R.P. and Stevenson, C.N., "Kinematics of Robot Wrists," *International Journal of Robotics Research*, Vol. 2, No. 1, 1985, pp. 31–38.

[15] Roth, B., "Performance Evaluation of Manipulators from a Kinematic Viewpoint", *National Bureau of Standards Workshop on Performance Evaluation on Programmable Robots and Manipulators*, National Bureau of Standards, NBS SP-459, 1976, pp. 39–61.

[16] Salisbury, J.K. and Craig, J.J., "Articulated Hands: Kinematic and Force Control Issues", *International Journal of Robotics Research*, Vol. 1, No. 1, 1982, pp. 4–17.

[17] Shimano, B., *The Kinematic Design and Force Control of Computer Controlled Manipulators*, Stanford A. I. Lab. Memo 313, March 1978.

[18] Slotine, J.J. and Khatib, O., Robust Control in Operational Space for Goal Positioned Manipulator Task.", *The 1986 American Control Conference*, Seattle, 1986.

[19] Yoshikawa, T., "Analysis and Control of Robot Manipulators with Redundancy", *Proceedings of the 1st International Symposium of Robotics Research*, MIT Press, Cambridge, MA, 1983, pp. 735–747.

]20] Yoshikawa, T., "Dynamic Manipulability of Robot Manipulators", *Proceedings 1985 IEEE International Conference on Robotics and Automation*, St. Louis, March 1985, pp. 1033–1038.

O. Khatib received the degree of "Docteur-Ingénieur en Automatique et Système" in 1980 from "l'École Nationale Supérieure de l'Aéronautique et de l'Espace," Toulouse, France. He is a Senior Research Associate at the Artificial Intelligence Laboratory, Stanford University. He has worked in the field of Robotics since 1976, when he joined "le Centre d'Étude et de Recherche de Toulouse." There, he developed the foundation of the operational space formulation and the artificial potential field concept for robot manipulator control and collision avoidance. Since 1981, his research at Stanford University was aimed at extending these methodologies to establish a unified framework for motion and active force control of robot manipulators operating in a cluttered and evolving environment. His research interest include issues of task description, constrained motion and force control, force strategies, redundancy, kinematic singularities, real-time obstacle avoidance, sensor fusion and high level programming systems. His is also concerned with the analysis and design of high-performance force-controlled robot manipulator and micro-manipulator systems.

J. Burdick is pursuing a Ph.D. in Mechanical Engineering at Stanford University, with expected completion in August 1987. Joel received his B.S. in Mechanical Engineering at Stanford in 1982. His research interests are in the design and control of robot manipulators, particularly redundant manipulators.